

ρ -meson self-energy and dielectron emissivity in an isospin-asymmetric pion medium

A. I. Titov and T. I. Gulamov*

Bogoliubov Theoretical Laboratory, Joint Institute for Nuclear Research, 141980 Dubna, Russia

B. Kämpfer

*Research Center Rossendorf, Institute for Nuclear and Hadron Physics, PF 510119, 01314 Dresden, Germany
and Institute for Theoretical Physics, Technical University Dresden, Mommsenstr. 13, 01062 Dresden, Germany*

(Received 21 July 1995)

The ρ -meson self-energy in an isospin-asymmetric pion gas at finite temperature and charged-pion chemical potential is evaluated. We utilize a conventional effective π - ρ Lagrangian and the functional integral representation of the partition function in the second order in the $\rho\pi\pi$ coupling constant. We analyze the ρ -meson polarization operator and its dependence on the invariant mass M and spatial momentum $|\mathbf{p}|$ of the ρ meson. The pole positions and the values of the imaginary parts of the self-energy for different polarization states have different functional dependences on M and $|\mathbf{p}|$. The corresponding dielectron rate (calculated from the imaginary part of the in-medium ρ -meson propagator) shows a distinctive asymmetry when the momentum $\mathbf{t} = \mathbf{p}_+ - \mathbf{p}_-$ is perpendicular or parallel to \mathbf{p} , where \mathbf{p}_\pm are the e^\pm momenta of the electron pair.

PACS number(s): 12.40.Vv, 11.10.Wx, 25.75.-q

I. INTRODUCTION

The intriguing question for modifications of hadron properties in hot and dense nuclear matter is currently an interesting problem in the realm of relativistic heavy-ion collisions and has been addressed by many authors. Most investigations focus on the temperature dependence of hadron masses and widths. In addition to other aspects, the ρ -meson dynamics is crucially important here because it may be related directly to observables. According to the vector dominance model [1] the pion electromagnetic form factor is almost completely dominated by the ρ meson below an invariant mass of about 1 GeV [2]. So can one hope to explore in-medium properties of the ρ meson via the dilepton production in the $\pi^+\pi^-$ annihilation process [3] in the course of heavy-ion collisions.

The investigation of the ρ -meson properties in dense and hot matter is quite ambitious, especially in the region below the chiral phase transition. Above the critical temperature, which probably coincides with the deconfinement temperature, the ρ meson should disappear from the hadronic spectrum of excitations as found in both the chiral mean field models [3] and lattice calculations [4]. The details of predicted ρ meson properties below the chiral phase transition depend on the physical picture of the matter constituents and their interactions with the ρ meson [5]. The models based on quark degrees of freedom, such as QCD lattice calculations in quenched approximation [6], QCD sum rules [7], the effective Lagrangians of the Nambu–Jona-Lasinio–type [8], or the models based entirely on the hadronic degrees of freedom [9–11] result in partially different predictions of the in-medium effects.

For an understanding of the role of conventional hadronic

interactions for the ρ meson modification under extreme conditions, it seems to be appropriate to study first the simplest model system of strongly interacting matter: a dense and hot pion gas with a small or negligible baryon admixture; such a matter state is often expected to be produced in the central region in ultrarelativistic heavy-ion collisions. This can be considered as background for more complete models (which should include also the baryonic degrees of freedom in case of intermediate-energy and relativistic heavy-ion collisions) and for more exotic interparticle interaction types.

Gale and Kapusta [12] have analyzed the temperature modification of the ρ -meson self-energy in the one-loop order (order g_ρ^2 in the coupling constant) at vanishing pion chemical potential. They found a modest increase of the ρ width and mass with temperature; this means that if a high energy experiment would show a substantial modification of the dilepton spectrum with an invariant mass in the ρ region, it could be considered as some indication of a more exotic process.

The model of Gale and Kapusta is extended by Koch [13] who considers the pion system in a chemical non-equilibrium state described by a positive chemical potential μ_π . The chemical potential is associated with the total pion density of the pion gas, and it is supposed that μ_π has the same value for π^+ and π^- . Previously, this idea has been put forward by Kataja and Ruuskanen [14] as an explanation of the observed enhancement of pions at low transverse momentum in relativistic heavy-ion collisions [15] as a consequence of the Bose-Einstein statistics. In Ref. [13], it is found that the incorporation of the pion chemical potential μ_π gives a strong enhancement of the muon pair yield in the low invariant mass region, provided the lepton pairs are produced predominantly via pion annihilation. This might serve as explanation of the so-called dilepton excess [16] observed in the present CERN Super Proton Synchrotron (SPS) heavy-ion experiments [17].

In principle, one needs to consider an additional degree of

*Permanent address: Physical and Technical Institute of Uzbek Academy of Sciences, 700084 Tashkent, Republic Uzbekistan.

freedom in the conventional ρ - π dynamics, namely a possible nonzero total electric or isospin charge of the pionic system. Because of the presence of other charged particles there may be a pronounced π^+ - π^- asymmetry. Some experimental data [18] and theoretical investigations [19] indeed point to this possibility. It may be a consequence of the proton-neutron asymmetry of the colliding heavy ions, which increases with increasing atomic weight of the colliding ions. (For example, new experimental data for Au + Au collisions at 1 GeV per nucleon points to values from 2 to 0.7 for the ratio of π^- to π^+ multiplicities depending on the pion energy [20].) The electric charge of a pionic system is controlled by the charge chemical potential μ_Q , which must not be confused with the chemical potential used by Koch [13] $\mu_\pi = \mu_\pi^0$. The latter one is a measure of the chemical equilibrium breaking. Instead, the chemical potentials for positive and negative pions are $\mu_{\pi^\pm} = \mu_\pi^0 \pm \mu_Q$.

The incorporation of the potential μ_Q into the theory leads to some nontrivial effects as, for example, the dilepton enhancement at invariant mass $2m_\pi$ [21], or a strong modification of the Goldstone modes [22].

Here, we explore this additional degree of freedom $\mu_Q \neq 0$. Our aim is an extension of the results of Gale and Kapusta [12] to the ρ -meson self-energy at finite temperatures and finite values of the chemical potential μ_Q . The role of baryonic degrees of freedom and the estimate of the dynamics of the isospin asymmetry are beyond the scope of our current consideration. Despite such simplifications we believe that our work may be considered as a necessary part of a more complete theory of the π - ρ subcomponent in a hot and dense baryonic isospin-asymmetric environment.

In our recent work [23], we restricted ourselves to the simplest case when the vector field, describing the ρ -meson, is considered in its rest frame with momentum $\mathbf{p}=0$. In such a case we find a weak increase of both the ρ -meson mass and the width with increasing temperature and chemical potential μ_Q . In the present paper we generalize our approach to an arbitrary finite value of the ρ -meson momentum. We evaluate the ρ -meson self-energy by using, as a starting point, a conventional effective π - ρ Lagrangian and the functional integral representation for the partition function, which is familiar from the relativistic quantum field theory at finite temperature and charge chemical potential. We take care of the transversality of the ρ polarization operator and analyze its dependence on the invariant mass M and the spatial momentum $|\mathbf{p}|$ of the ρ meson. We show that this dependence leads to a noticeable modification of the shape of the thermal dilepton production rate, which we calculate from the imaginary part of the polarization operator. Moreover, at large values of μ_Q we find for different polarization states a distinctive difference in the pole positions and in the values of the imaginary parts of the self-energy as functions of M and $|\mathbf{p}|$. This leads to a pronounced asymmetry of the dielectron production rate when the momentum $\mathbf{t}=\mathbf{p}_+-\mathbf{p}_-$ is perpendicular or parallel to \mathbf{p} , where \mathbf{p}_\pm are the e^\pm momenta of the electron pair. This nontrivial in-medium effect can be, in principle, verified experimentally with sufficient accuracy.

Our paper is organized as follows. In Sec. II we present the functional representation of our π - ρ model system. In

Sec. III we evaluate the ρ -meson self-energy in one-loop order at finite temperature and chemical potential μ_Q . The ρ -meson self-energy is analyzed in Sec. IV. With this at hand we calculate in Sec. V the dilepton rate from the imaginary part of the in-medium ρ -meson propagator and discuss the asymmetry for different polarizations. The summary can be found in Sec. VI.

II. THE MODEL

Our starting point is the effective Lagrangian \mathcal{L} which describes a system of charged pions and neutral vector ρ mesons by

$$\mathcal{L} = \frac{1}{2} (D^\nu \phi)^* D_\nu \phi - \frac{1}{2} m_\pi^2 \phi \phi^* - \frac{1}{4} \rho_{\mu\nu} \rho^{\mu\nu} + \frac{1}{2} m_\rho^2 \rho^2, \quad (1)$$

where ϕ is the complex charged pion field, ρ stands for the vector field with the strength $\rho_{\mu\nu} = \partial_\mu \rho_\nu - \partial_\nu \rho_\mu$, and $D_\nu = \partial_\nu - ig_\rho \rho_\nu$ is the covariant derivative; μ and ν are Lorentz indices. The Hamiltonian of the system is related to the Lagrangian of Eq. (1) in the usual way:

$$\mathcal{H} = \frac{\partial \mathcal{L}}{\partial(\partial_0 \varphi)} \partial_0 \varphi - \mathcal{L} \quad (2)$$

with $\varphi = (\phi, \phi^*, \rho)$. The reference for what follows at finite temperature $T \neq 0$ and $\mu_{\pi^\pm} = 0$ is the paper of Gale and Kapusta [12].

Let us consider now the case when the system admits some conserved electric or isospin charge. We focus on the case $\mu_\pi^0 = 0$ and concentrate on the incorporation of μ_Q . A finite value of the chemical potential μ_Q leads to a transformation of the Hamiltonian which we use for the calculation of the partition function

$$\mathcal{H} \rightarrow \mathcal{H} - \mu_Q J_0, \quad (3)$$

where J_0 is the time component of Noether's current

$$J_\nu \equiv i \frac{1}{2} [\phi^* D_\nu \phi - \phi (D_\nu \phi)^*]. \quad (4)$$

The ρ -meson propagator D in a medium may be obtained from the partition function with a functional integral representation of the form [24,25]

$$\mathcal{Z} = \int \mathcal{D}\pi_\varphi \int_{\text{periodic}} \mathcal{D}\varphi \times \exp \left\{ \int_0^\beta d\tau \int_V d\mathbf{x} \left(i \pi_\varphi \frac{\partial \varphi}{\partial \tau} - \mathcal{H} + \mu_Q J_0 \right) \right\},$$

where $\pi_\varphi = \partial \mathcal{L} / \partial(\partial_0 \varphi)$ are the conjugate momenta to φ . The integration over π_φ gives

$$\mathcal{Z} = \int_{\text{periodic}} \tilde{\mathcal{D}}\rho \mathcal{D}\phi \mathcal{D}\phi^* e^{S_0 + S_{\text{int}}}, \quad (5)$$

where $S_0 = S_{0\pi} + S_{0\rho}$ describes the noninteracting part of the total effective action, and S_{int} corresponds to the interaction part: i.e.,

$$\begin{aligned} S_{0\pi} &= \int_0^\beta d\tau \int_V d\mathbf{x} \left[\frac{1}{2} |\partial\phi|^2 - \frac{1}{2} (m_\pi^2 - \mu_Q^2) |\phi|^2 - \mu_Q j_0 \right], \\ S_{0\rho} &= \int_0^\beta d\tau \int_V d\mathbf{x} \left(-\frac{1}{4} \rho_{\mu\nu} \rho^{\mu\nu} + \frac{1}{2} m_\rho^2 \rho^2 - \frac{1}{2\alpha} (\partial_\mu \rho^\mu)^2 \right), \\ S_{\text{int}} &= \int_0^\beta d\tau \int_V d\mathbf{x} \left[\frac{1}{2} g_\rho^2 \rho^2 |\phi|^2 + g_\rho (\rho_\mu j^\mu + \mu_Q \rho_0 |\phi|^2) \right], \end{aligned} \quad (6)$$

where $\tilde{\mathcal{D}}\rho = \mathcal{D}\rho \cdot \det(\partial_4)$ [with $\det\partial_4 \equiv \det(\partial\partial_\mu\rho^\mu/\partial\rho_4)$] and $j_\mu = i/2(\phi^* \partial_\mu \phi - \phi \partial_\mu \phi^*)$, $i\partial_0 = \partial_\tau$, $\rho_0 = i\rho_4$, etc. $S_{0\rho}$ includes the gauge fixing term with $\alpha \rightarrow 0$, which insures that only those vector field configurations with $\partial_\mu \rho^\mu = 0$ contribute to the partition function.

Expanding Eq. (5) in power series in S_{int} and taking the logarithm of both sides, we get, in the second order of g_ρ ,

$$\begin{aligned} \ln \mathcal{Z} &= \ln \mathcal{Z}_0 + \ln \mathcal{Z}_{\text{int}}, \\ \ln \mathcal{Z}_{\text{int}} &\simeq \frac{1}{2} g_\rho^2 \left\langle \left\langle \int d\tau d\mathbf{x} \rho^2 |\phi|^2 \right\rangle_0 \right. \\ &\quad \left. + \left\langle \left\langle \int d\tau d\mathbf{x} (\rho_\nu j_\nu + \mu_Q \rho_0 |\phi|^2) \right\rangle_0^2 \right\rangle, \end{aligned} \quad (7)$$

where

$$\mathcal{Z}_0 = \int \mathcal{D}\varphi e^{S_0}, \quad \langle R \rangle_0 \equiv \mathcal{Z}_0^{-1} \int \mathcal{D}\varphi R e^{S_0}. \quad (8)$$

The full ρ propagator may be obtained with the help of Dyson's equation

$$(D^{-1})^{\mu\nu} = (D_0^{-1})^{\mu\nu} + \Pi^{\mu\nu}, \quad (9)$$

where $D_0^{\mu\nu}$ is the free propagator defined by $S_{0\rho}$, and the polarization operator $\Pi_{\mu\nu}$ is related to a functional derivative of the partition function as

$$\Pi_{\mu\nu} = -2 \frac{\delta \ln \mathcal{Z}_{\text{int}}}{\delta D_0^{\mu\nu}}. \quad (10)$$

III. THE ρ -MESON PROPAGATOR

The calculation of $\ln \mathcal{Z}_{\text{int}}$ may be performed by utilizing the methods of Ref. [24] and textbook recipes [25]. After some tedious algebraic exercises we get the following expression for $\Pi_{\mu\nu}$:

$$g_\rho^{-2} \Pi^{\mu\nu}(\mu_Q, p) = \delta^{\mu\nu} I_1 - \frac{1}{4} I_2^{\mu\nu} + 4\mu_Q (\delta_4^\mu I_3^\nu + \delta_4^\nu I_3^\mu), \quad (11)$$

where

$$\begin{aligned} I_1 &= T \sum_{k_4} \int \frac{d^3\mathbf{k}}{(2\pi)^3} \frac{\delta^{\mu\nu}}{A(k)} \left(1 + \frac{A(k)^2 - B(k)^2}{A(k)^2 + B(k)^2} \right), \\ I_2^{\mu\nu} &= T \sum_{k_4} \int \frac{d^3\mathbf{k}}{(2\pi)^3} \frac{4k^\mu k^\nu - 4\delta_4^\mu \delta_4^\nu \mu_Q^2}{A_+ A_-} [1 + \mathcal{F}(\mu_Q, p, k)], \\ I_3^\nu &= T \sum_{k_4} \int \frac{d^3\mathbf{k}}{(2\pi)^3} k^\nu \frac{B_+ A_- + B_- A_+}{(A_+^2 + B_+^2)(A_-^2 + B_-^2)}. \end{aligned} \quad (12)$$

In the above, the fourth component of the momentum four-vectors is the Matsubara frequency, i.e., k_4 or $p_4 = 2\pi T \times \text{integer}$. The functions A_\pm and B_\pm depend on the chemical potential as

$$A_\pm = (k_4 \pm \frac{1}{2} p_4)^2 + \omega_\pm^2 - \mu_Q^2, \quad B_\pm = -2\mu_Q (k_4 \pm \frac{1}{2} p_4), \quad \omega_\pm^2 = (\mathbf{k} \pm \frac{1}{2} \mathbf{p})^2 + m_\pi^2,$$

and $A(k) = A_\pm(p=0)$, $B(k) = B_\pm(p=0)$. The function $\mathcal{F}(\mu_Q, p, k)$ is a combination of A_\pm and B_\pm :

$$\mathcal{F}(\mu_Q, p, k) = \frac{A_+^2 - B_+^2}{A_+^2 + B_+^2} + \frac{A_-^2 - B_-^2}{A_-^2 + B_-^2} + \frac{(A_+^2 - B_+^2)(A_-^2 - B_-^2) - 4A_+ A_- B_+ B_-}{(A_+^2 + B_+^2)(A_-^2 + B_-^2)}.$$

In the limit of $\mu_Q = 0$, Eq. (11) reduces to the self-energy of Ref. [12], obtained within the framework of finite-temperature Feynman rules. We calculate the self-energy of Eq. (11) by utilizing the standard technique, i.e., the discrete summation is replaced by the contour integral [25,26].

The first term, I_1 , in Eqs. (12) does not depend on the external momentum p , and its calculation gives

$$I_1 = 2 \int \frac{d^3\mathbf{k}}{(2\pi)^3} \frac{1}{2\omega} [1 + N(\omega)], \quad (13)$$

where $N(\omega) = n(\omega + \mu_Q) + n(\omega - \mu_Q)$, $n(\omega) = (e^{\omega/T} - 1)^{-1}$, and $\omega^2 = \mathbf{k}^2 + m_\pi^2$. Calculating $I_2^{\mu\nu}$ and I_3^ν we see that only the poles located at $k_0 = a_{1,2}$ and $b_{1,2}$ with

$$a_{1,2} = \omega_\pm \pm \mu_Q - \frac{1}{2} i p_4, \quad b_{1,2} = \omega_\pm \pm \mu_Q + \frac{1}{2} i p_4,$$

contribute to the contour integral. For example, the contributions to $I_2^{4,4}$ and I_3^4 stemming from a_1 yield

$$I_{2,a_1}^{4,4} = 2 \int \frac{d^3\mathbf{k}}{(2\pi)^3} \frac{4(k_0^2 + \mu_Q^2)}{\omega_+} \frac{1}{(\omega_+ - p_0)^2 - \omega_-^2} \left\{ \frac{1}{2} + n(k_0) \right\}_{k_0=a_1},$$

$$I_{3,a_1}^{(4)} = 2 \int \frac{d^3\mathbf{k}}{(2\pi)^3} \frac{k_0}{4\omega_+} \frac{1}{(\omega_+ - p_0)^2 - \omega_-^2} \left\{ \frac{1}{2} + n(k_0) \right\}_{k_0=a_1},$$

and their contributions to $g_\rho^{-2} \Pi^{\mu\nu}(\mu_Q, p)$ in Eq. (11) result in

$$-\frac{1}{4} I_{2,a_1}^{4,4} + 8\mu_Q I_{3,a_1}^{(4)} = 2 \int \frac{d^3\mathbf{k}}{(2\pi)^3} \left\{ -\frac{k_0^2 + \mu_Q^2}{\omega_+} + \frac{2k_0\mu_Q}{\omega_+} \right\} \frac{1}{(\omega_+ - p_0)^2 - \omega_-^2} \left\{ \frac{1}{2} + n(k_0) \right\}_{k_0=a_1}$$

$$= -2 \int \frac{d^3\mathbf{k}}{(2\pi)^3} \frac{1}{\omega_+} \frac{(\omega_+ - p_0/2)^2}{(\omega_+ - p_0)^2 - \omega_-^2} \left\{ \frac{1}{2} + n(\omega_+ + \mu_Q) \right\}$$

($p_0 = ip_4$). The final result for the components of $\Pi^{\mu\nu}$ is

$$\Pi^{44} = -\frac{g_\rho^2}{(2\pi)^2} \int_0^\infty k^2 dk \left\{ \frac{4\omega^2 - p_4^2}{4kq} \ln(a) + \frac{ip_4\omega}{kq} \ln(b) - 2 \right\} \{1 + N(\omega)\},$$

$$\Pi^{4j} = -\frac{p_4 p^j}{\mathbf{p}^2} \Pi^{44},$$

$$\Pi^{ij} = \delta^{ij} \mathcal{A} + \frac{p^i p^j}{\mathbf{p}^2} \mathcal{B}, \quad (14)$$

where

$$a = \frac{(p_4^2 + \mathbf{p}^2 - 2k|\mathbf{p}|)^2 + 4p_4^2\omega^2}{(p_4^2 + \mathbf{p}^2 + 2k|\mathbf{p}|)^2 + 4p_4^2\omega^2}, \quad b = \frac{(p_4^2 + \mathbf{p}^2)^2 - 4(ip_4\omega + 2k|\mathbf{p}|)^2}{(p_4^2 + \mathbf{p}^2)^2 - 4(ip_4\omega - 2k|\mathbf{p}|)^2},$$

$$\mathcal{A} = -\frac{1}{2} \frac{g_\rho^2}{4\pi^2} \int_0^\infty k^2 dk \left(\frac{2(p_4^2 - \mathbf{p}^2)}{\mathbf{p}^2} - \frac{ip_4\omega(p_4^2 + \mathbf{p}^2)}{k|\mathbf{p}|^3} \ln(b) + \frac{p_4^2(p_4^2 - 4\omega^2) - \mathbf{p}^2(4k^2 - \mathbf{p}^2 - 2p_4^2)}{4k|\mathbf{p}|^3} \ln(a) \right) \{1 + N(\omega)\},$$

$$\mathcal{B} = -\frac{1}{2} \frac{g_\rho^2}{4\pi^2} \int_0^\infty k^2 dk \left(-\frac{2(3p_4^2 - \mathbf{p}^2)}{\mathbf{p}^2} + \frac{ip_4\omega(\mathbf{p}^2 + 3p_4^2)}{k|\mathbf{p}|^3} \ln(b) - \frac{3p_4^2(p_4^2 - 4\omega^2) - \mathbf{p}^2(4k^2 - 2p_4^2 - \mathbf{p}^2)}{4k|\mathbf{p}|^3} \ln(a) \right) \{1 + N(\omega)\}. \quad (15)$$

One observes that all the dependence on the chemical potential μ_Q and the temperature T is absorbed into the Bose factor $N(\omega)$. The substitution of

$$\frac{1}{2} \{n(\omega + \mu_Q) + n(\omega - \mu_Q)\} \rightarrow n(\omega)$$

in the above equations reproduces the results of Ref. [12].

In Minkowski space the self-energy $\Pi^{\mu\nu}$ may be expressed in the form

$$\Pi^{\mu\nu} = F P_L^{\mu\nu} + G P_T^{\mu\nu}, \quad (16)$$

where G and F are the so-called longitudinal and transverse

masses, and $P_L^{\mu\nu}$ and $P_T^{\mu\nu}$ are the longitudinal and transverse projection tensors:

$$P_T^{00} = P_T^{0i} = P_T^{i0} = 0, \quad P_T^{ij} = \delta^{ij} - p^i p^j / \mathbf{p}^2,$$

$$P_L^{\mu\nu} = p^\mu p^\nu / p^2 - g^{\mu\nu} - P_T^{\mu\nu}. \quad (17)$$

The tensor structure of $P_L^{\mu\nu}$ and $P_T^{\mu\nu}$ results in the transversality of $\Pi^{\mu\nu}$ with respect to the external momentum which confirms the current conservation. The final expression of the in-medium ρ propagator reads

$$D^{\mu\nu} = -\frac{P_L^{\mu\nu}}{p^2 - m_\rho^2 - F} - \frac{P_T^{\mu\nu}}{p^2 - m_\rho^2 - G} + \alpha \frac{p^\mu p^\nu}{p^2(p^2 - \alpha m_\rho^2)}_{\alpha \rightarrow 0}. \quad (18)$$

In the limit $T=0, \mu_Q=0, G=F=0$, $D^{\mu\nu}$ is reduced to the conventional vector meson propagator [25,27,28].

For applications we must perform an analytical continuation from the discrete Matsubara frequencies to the

Minkowski space, i.e., $p_0=ip_4 \rightarrow p_0=E+i\delta$, and calculate the divergent part of the self-energy, and regularize it with counterterms. We use the dimensional regularization as in Refs. [12,23] and find

$$\begin{aligned} \text{Re}F_{\text{vac}}(M^2) = \text{Re}G_{\text{vac}}(M^2) &= \frac{g_\rho^2}{48\pi^2} \left(M^2 (1 - 4m_\pi^2 M^{-2})^{3/2} \ln \left\{ \frac{1 + (1 - 4m_\pi^2 M^{-2})^{1/2}}{1 - (1 - 4m_\pi^2 M^{-2})^{1/2}} \right\} + 8m_\pi^2 + CM^2 \right), \\ C &= - \left(1 - \frac{4m_\pi^2}{m_\rho^2} \right)^{3/2} \ln \left(\frac{(1 - 4m_\pi^2/m_\rho^2)^{1/2} + 1}{(1 - 4m_\pi^2/m_\rho^2)^{1/2} - 1} \right) - \frac{8m_\pi^2}{m_\rho^2}, \end{aligned} \quad (19)$$

$$\text{Im}F_{\text{vac}}(M^2) = \text{Im}G_{\text{vac}}(M^2) = - \frac{g_\rho^2}{48\pi^2} M^2 (1 - 4m_\pi^2 M^{-2})^{3/2} \Theta(M^2 - 4m_\pi^2), \quad (20)$$

$$\begin{aligned} \text{Re}G_{\text{mat}} &= \frac{g_\rho^2}{8\pi^2} \int_0^\infty k^2 dk \frac{N(\omega)}{\omega} f_{G,R}(|\mathbf{p}|, M, \omega), \\ \text{Re}F_{\text{mat}} &= \frac{g_\rho^2}{8\pi^2} \int_0^\infty k^2 dk \frac{N(\omega)}{\omega} f_{F,R}(|\mathbf{p}|, M, \omega), \\ \text{Im}G_{\text{mat}} &= \frac{g_\rho^2}{8\pi} \int_0^\infty k^2 dk \frac{N(\omega)}{\omega} f_{G,I}(|\mathbf{p}|, \mathbf{M}, \omega), \end{aligned} \quad (21)$$

$$\text{Im}F_{\text{mat}} = \frac{g_\rho^2}{8\pi} \int_0^\infty k^2 dk \frac{N(\omega)}{\omega} f_{F,I}(|\mathbf{p}|, M, \omega); \quad (22)$$

where the functions $f \dots$ in the integrands read

$$\begin{aligned} f_{G,R}(|\mathbf{p}|, M, \omega) &= \frac{2(E^2 + \mathbf{p}^2)}{\mathbf{p}^2} - \frac{M^2 E \omega}{k|\mathbf{p}|^3} \ln|b| - \frac{E^2(4\omega^2 + E^2) - \mathbf{p}^2(4k^2 - \mathbf{p}^2 + 2E^2)}{4k|\mathbf{p}|^3} \ln|a|, \\ f_{F,R}(|\mathbf{p}|, M, \omega) &= \frac{M^2}{k|\mathbf{p}|^3} \left[\frac{4\omega^2 + E^2}{2} \ln|a| + 2E\omega \ln|b| - 4 \right], \\ f_{G,I}(|\mathbf{p}|, M, \omega) &= \frac{E^2(4\omega^2 + E^2) - \mathbf{p}^2(4k^2 - \mathbf{p}^2 + 2E^2) - 4M^2 E \omega}{4k|\mathbf{p}|^3} \zeta, \\ f_{F,I}(|\mathbf{p}|, M, \omega) &= - \frac{M^2(2\omega - E)^2}{2k|\mathbf{p}|^3} \zeta, \end{aligned} \quad (23)$$

and we have introduced the abbreviation $\zeta = \Theta(k - k_-) \cdot \Theta(k_+ - k)$ with $2k_\pm = |E(1 - 4m_\pi^2/M^2)^{1/2} \pm |\mathbf{p}||$. The subscripts “mat” and “vac” denote the matter dependent contributions at finite values of T and μ_Q , and the vacuum contributions at $T=0$ and $\mu_Q=0$, respectively.

The above expressions show the physical origin of the differences between F and G . In the vacuum there is no preferred rest frame, i.e., the polarization operator $\Pi^{\mu\nu}$ is proportional to $g^{\mu\nu}p^2 - p^\mu p^\nu$, and the equality $F=G$ holds with F and G depending only on p^2 . At finite temperature and density we must take into account the particle distribution functions which depend on the reference frame. These particle distributions now define a preferred local rest frame. This means that the form factors F and G depend on the ρ

energy E and spatial ρ momentum \mathbf{p} separately. More explicitly, a noncovariant decomposition of the self-energy in Eq. (16) in the medium’s rest frame leads to a difference in the integrand functions f_F and f_G in Eq. (23) which are defined completely by the form of the projection operators $P_{L,T}^{\mu,\nu}$, and also $f_{F,G}$ depends separately on E and \mathbf{p} . At fixed values of M (or E) and \mathbf{p} they have a different dependence on ω . In the nonrealistic case of $N(\omega) = \text{const}$ this difference is not essential because the corresponding integrals for F and G are equal to each other and one obtains $F_{\text{mat}} = G_{\text{mat}}$. But in the realistic case in a medium with preferred rest frame the distribution functions $N(\omega)$ deform the integrands and result in a difference of F_{mat} and G_{mat} . The influence of $N(\omega)$ in

creases with the temperature and the chemical potential and, moreover, its role is growing with increasing values of $|\mathbf{p}|$.

IV. THE ρ -MESON SELF-ENERGY

From the above we see that the in-medium effects manifest themselves in (i) the shift of pole position of the ρ -meson propagator because of modification of the real part of the self-energy, (ii) the modification of the imaginary part of the self-energy, which is responsible for the decay width, and (iii) the differences in the differences of the real and imaginary parts for different polarizations. All these phenomena depend on T , and μ_Q , and the ρ -meson momentum. At large values of the spatial momentum $|\mathbf{p}|$ all medium corrections vanish because this case corresponds to short range correlations, where the many-body effects become rather small. At $|\mathbf{p}|=0$ we have no preferential direction and the directional differences in (i) and (ii) disappear.

The matter corrections as functions of T and $|\mathbf{p}|$ at $\mu_Q=0$ have been studied in Ref. [12]. There it is shown that the corrections decrease rapidly with decreasing temperature T . So we focus on large values of T . In our calculations we use $m_\pi=139.6$ MeV, $m_\rho=770$ MeV, and $g_\rho^2/4\pi=2.93$.

Let us first discuss the dispersion relation, i.e., the dependence of the ρ energy on the spatial momentum. In the medium, this dependence is different from that in the case of the free meson, $\omega_{\rho 0}^2=m_\rho^2+\mathbf{p}^2$. Moreover, the dispersion relations are different for different polarization states: the longitudinal and transverse dispersions are defined by the functions $\text{Re}G(p_0, \mathbf{p})$ and $\text{Re}F(p_0, \mathbf{p})$, respectively, and are determined as solutions of the equations

$$\begin{aligned}\omega_L^2 &= \mathbf{p}^2 + m_\rho^2 + F_R(\omega_L, |\mathbf{p}|, T, \mu_Q), \\ \omega_T^2 &= \mathbf{p}^2 + m_\rho^2 + G_R(\omega_T, |\mathbf{p}|, T, \mu_Q).\end{aligned}\quad (24)$$

At $|\mathbf{p}|=0$, $\omega_{L,T}$ represent just the in-medium ρ mass.

In describing the matter modification for longitudinal and transverse dispersions it is more illustrative to specify the difference $\Delta\omega_{L,T}=\omega_{L,T}-\omega_{\rho 0}$ which is displayed in Fig. 1 for different values of the chemical potential $\mu_Q=0, 60, 120$ MeV at $T=150$ MeV. We find that (i) $\Delta\omega_{L,T}$ increase with increasing chemical potential, (ii) $\Delta\omega_{L,T}$ decrease with increasing momentum $|\mathbf{p}|$, and (iii) the matter modifications for different polarizations are similar in shape but they do not coincide exactly. Within the present conventional π - ρ dynamics model, as in other hadronic models too [11], an increasing in-medium mass is obtained. (This is at variance to the QCD-sum rules results which predict a decrease of all in-medium masses [5,7]; see, however, recent lattice calculations [6].) We find that extremely large values of $\mu_Q \approx 120$ MeV (which should be considered as an upper limit of the realistically expected values of μ_Q [23]) lead to corrections which are about twice as large as those at $\mu_Q=0$ (at the same temperature). Nevertheless, these in-medium corrections turn out as comparatively small, i.e., a 4% (10%) mass shift at $\mu_Q=0$ ($\mu_Q=120$ MeV) and $T=150$ MeV. These values appear compatible with the recent QCD lattice results [6].

In parallel with the dispersion relation it is interesting to look at the pole positions $M_{L,T}(\mathbf{p})$, defined by

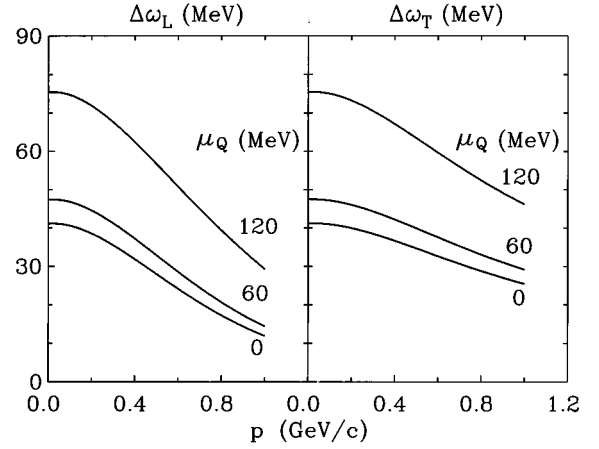


FIG. 1. The in-medium modifications of the longitudinal (left panel) and transverse (right panel) dispersion relations $\Delta\omega_{L,T}=\omega_{L,T}-\omega_0$ for various values of the chemical potential $\mu_Q=0,60,120$ MeV ($T=150$ MeV) as function of the momentum.

$M_{L,T}^2(\mathbf{p})=\omega_{L,T}^2(\mathbf{p})-\mathbf{p}^2$, which coincide with $\omega_{L,T}$ at $|\mathbf{p}|=0$. Figure 2 shows the difference of the shifts of the pole position $\Delta M_{L,T}=M_{L,T}-m_\rho$ for different polarization states. One observes that ΔM_L decreases faster with increasing values of $|\mathbf{p}|$. This is due to the inequality $\text{Re}F < \text{Re}G$ at $|\mathbf{p}| > 0$.

Figure 3 shows the dependence of the imaginary parts of the self-energy on the invariant mass M of the ρ meson at high temperature and for different values of μ_Q . We find increasing values of $\text{Im}G$ and $\text{Im}F$ with increasing mass M , which leads to an increase of the damping constants. We also find some difference between $\text{Im}F$ and $\text{Im}G$, given by Eqs. (22) and (21), where $|\text{Im}F| > |\text{Im}G|$ at finite values of $|\mathbf{p}|$. The largest difference is seen in the region of $M \sim 0.3-0.5$ GeV for finite values of $|\mathbf{p}|$. This is illustrated in Fig. 4 where the ratio $\text{Im}G/\text{Im}F$ as a function of M at different values of $|\mathbf{p}|$ and μ_Q is displayed. Here and in the following discussion we have restricted ourselves to the ex-

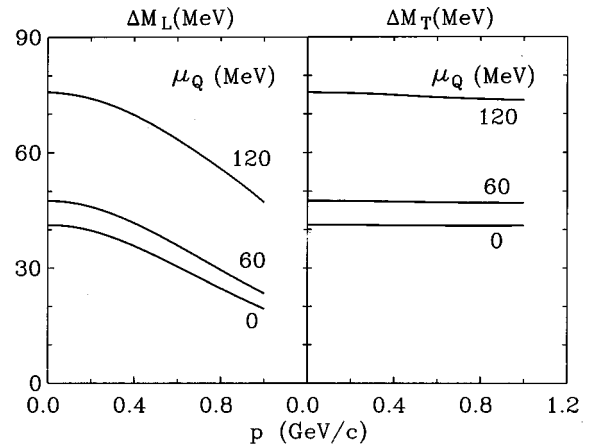


FIG. 2. The shift of the pole positions for different polarization states $\Delta M_{L,T}=M_{L,T}-m_\rho$ for various values of the chemical potential $\mu_Q=0,60,120$ MeV ($T=150$ MeV) as function of the momentum.

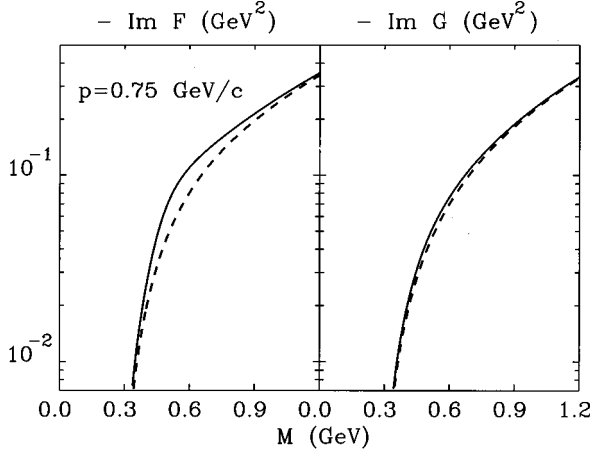


FIG. 3. The imaginary parts of the polarization operators $-\text{Im}F$ and $-\text{Im}G$ as functions of the invariant mass M at temperature $T=150$ MeV and ρ -meson momentum $|\mathbf{p}|=0.75$ GeV. Solid (dashed) curves depict $\mu_Q=120$ (0) MeV.

trime cases $\mu_Q=0$ and 120 MeV. In Ref. [23] a value of $\mu_Q \sim 60$ MeV is estimated for presently available experimental data. As seen in Figs. 1 and 2 such a value of μ_Q does not cause a dramatic effect. But without explicit calculations this statement cannot be anticipated.

V. THE THERMAL DILEPTON PRODUCTION RATE

Now we try to elucidate whether the predicted in-medium effects can be seen in the dielectron production rate. Let us first recall that the thermal dilepton production rate within the vector dominance model is related to the imaginary part of the ρ propagator as [12,29]

$$E_+ E_- \frac{dR}{d^3\mathbf{p}_+ d^3\mathbf{p}_-} = \frac{1}{(2\pi)^6} \frac{e^4 m_\rho^4}{g_\rho^2 M^2} [(1-\xi)W_L + (1+\xi)W_T] n(E), \quad (25)$$

with

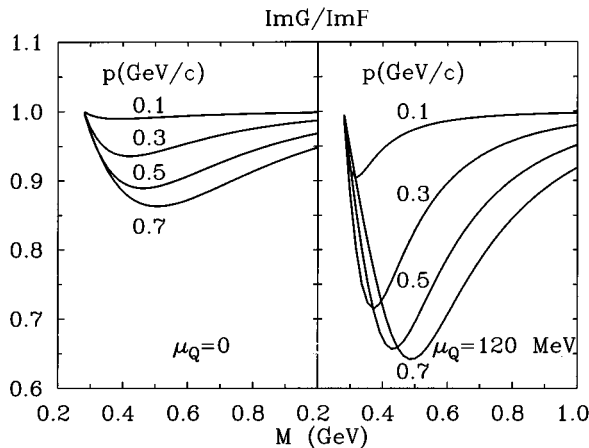


FIG. 4. The ratio $\text{Im}G/\text{Im}F$ as function of the invariant mass M for different values $|\mathbf{p}|$ and $\mu_Q=0$ and 120 MeV (left and right panels; $T=150$ MeV).

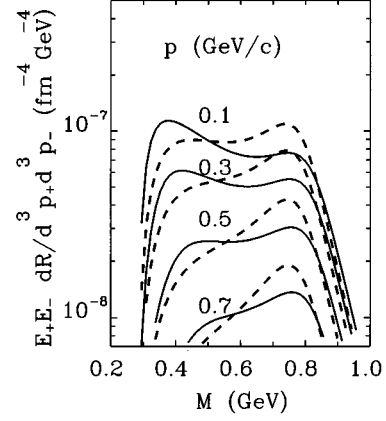


FIG. 5. The dielectron production rate for different total momenta p , as function of the invariant mass M ($T=150$ MeV; the dashed and solid curves are for $\mu_Q=0$ and 120 MeV, respectively).

$$\xi = 1 - \left(t^2 - \frac{(\mathbf{t} \cdot \mathbf{p})^2}{p^2} \right) M^{-2}, \quad (26)$$

$$W_L = \frac{-F_I}{(M^2 - m_\rho^2 - F_R)^2 + F_I^2},$$

$$W_T = \frac{-G_I}{(M^2 - m_\rho^2 - G_R)^2 + G_I^2}, \quad (27)$$

where $p=p_++p_-$ is the total pair momentum, $p=(E,\mathbf{p})$, $p^2=M^2$, and $t=p_+-p_-$. The function ξ depends on the angle between the vectors \mathbf{t} and \mathbf{p} and varies from 0 at $\theta_{\mathbf{t}\mathbf{p}}=\pi/2$ up to 1 at $\theta_{\mathbf{t}\mathbf{p}}=0$. Integrating Eq. (25) over the lepton directions we get the rate as function of the invariant mass as

$$\frac{dR}{dM} = \frac{1}{12\pi^4} \frac{e^4 m_\rho^4}{g_\rho^2} \int dE \sqrt{\frac{E^2}{M^2} - 1} (W_L + 2W_T) n(E). \quad (28)$$

Figure 5 shows the differential rate given by Eq. (25) as function of M at different values of $|\mathbf{p}|$ at $\xi=0$, where both the polarizations $W_{L,T}$ contribute with the same weight. This value of ξ corresponds to events where the leptons have equal energies, $E_+=E_-=E/2$, and the angle between their momenta is related to M and E by $\sin(\theta_{+-}/2)=M/E$. One can see that at small values of $|\mathbf{p}|$ the standard double-humped structure of the rate appears. The first bump is attributed to a combination of opening the available phase space at threshold and the suppression caused by the factor $n(\sqrt{M^2+\mathbf{p}^2}/T)/M^2$ in Eq. (25), while the second bump is the consequence of the resonancelike behavior of the rate. At large values of $|\mathbf{p}|$, the first bump is suppressed by the Bose factor $n(\sqrt{M^2+\mathbf{p}^2}/T)$, which leads to a suppression of the total rate as well. We also confirm the conclusion of Ref. [12] that the shape of the distribution at fixed $|\mathbf{p}|$ is not very sensitive variations of the temperature at $\mu_Q=0$.

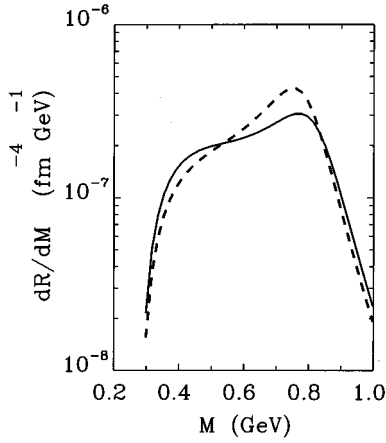


FIG. 6. The integrated dielectron production rate as function of the invariant mass M (notation as in Fig. 5).

At small values $|\mathbf{p}|$ there is no difference between the two polarizations, and the matter correction to the pole shift at finite values μ_Q is largest. Comparing the calculated distributions at different values μ_Q we find that the modification of the second bump position is probably too small to be verifiable experimentally in the spectra. However, we see a noticeable in-medium dependence of the rate shape. This is explained by the Bose factors being proportional to $[\exp\{(M/2 - \mu_Q)/T\} - 1]^{-1}$ in Eqs. (22), (21) which are most important at small values of M . At large values of $|\mathbf{p}|$ the difference of F_{mat} and G_{mat} leads to different contributions to the longitudinal and transverse polarizations and, as consequence, the net rate suffers an additional deformation.

Figure 6 shows the integrated rate as function of the invariant mass. We see that the shape is close to the shape of the differential rate in the region $|\mathbf{p}| = 0.3\text{--}0.4$ GeV which gives the largest contribution to the integral of Eq. (28). There is some effect of the finite potential μ_Q ; however, it seems hardly measurable. Note also that we display in Fig. 6 again the extreme cases $\mu_Q = 0$ vs 120 MeV. For the more realistic value $\mu_Q \sim 60$ MeV [23] the effect tends to vanish. As a rule, the temperature dependence of the rate is stronger than a chemical potential dependence [33].

The effect of the difference of the longitudinal and transverse polarization contributions manifests itself most clearly in the asymmetry of the differential distributions, which we define here by

$$A_{\perp\parallel} = \frac{dR(\mathbf{t}\perp\mathbf{p}) - dR(\mathbf{t}\parallel\mathbf{p})}{dR(\mathbf{t}\perp\mathbf{p})} = \frac{W_L - W_T}{W_L + W_T} \quad (29)$$

(other definitions are also possible [34]). This asymmetry is displayed in Fig. 7. At small values of $|\mathbf{p}|$ one gets $W_L \approx W_T$, and the asymmetry vanishes. In the case of finite values of \mathbf{p} , we find $A_{\perp\parallel} \rightarrow 0.5(\Delta M_T^2 - \Delta M_L^2)/m_\rho^2 \approx 0$ $M \rightarrow 2m_\pi$. On the other hand, one can see that $A_{\perp\parallel}$ has a second zero at $M \approx m_\rho + \delta(\mathbf{p})$, where $\delta(\mathbf{p})$ is a smoothly decreasing function of \mathbf{p}^2 with $\delta(\mathbf{p})/m_\rho < 10^{-2}$. So, the asymmetry reaches a maximum between the two zeros $2m_\pi < M < m_\rho$ because of $\text{Im}G < \text{Im}F$ at $M < m_\rho$. We find that the asymmetry $A_{\perp\parallel}$ increases with $|\mathbf{p}|$, and it may be as large as 0.25 for $\mu_Q = 120$ MeV, whereas at $\mu_Q = 0$ it is

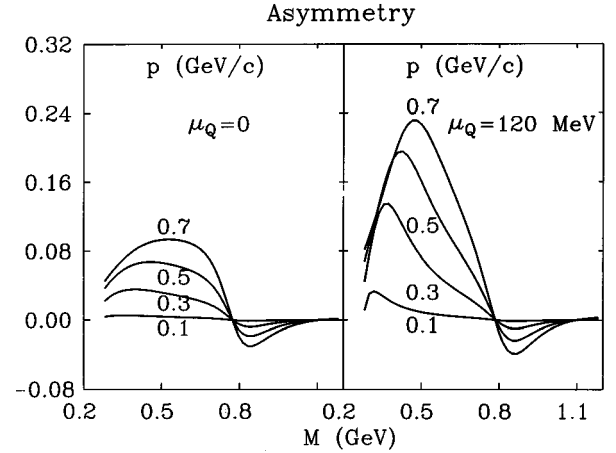


FIG. 7. The asymmetry $A_{\perp\parallel}$ as function of the invariant mass M for different values $|\mathbf{p}|$ and for $\mu_Q = 0$ and 120 MeV (left and right panels; $T = 150$ MeV).

about 2.5 times smaller. For the more realistic value $\mu_Q \sim 60$ MeV the asymmetry reaches its maximum value 0.13 at $M = 500$ MeV; i.e., there is also a verifiable effect on the 20% level compared to $\mu_Q = 0$.

Probably, this is the most interesting in-medium effect of our consideration which can provide a fresh insight into the dilepton production as a probe for the hadron properties at extreme conditions. Note, however, that the presence of other mesons and baryons needs to be regarded for more firm quantitative predictions.

An important question is whether the predicted effect is experimentally accessible. In the present stage of our investigations, our goal is to point out that it might be clearly observable on the level of 15–25%. The feasibility of the idea depends on the experimentalist's art and power to reach it. Known examples from different fields of particle and nuclear physics show that such asymmetries might be measured with high accuracy on the level of a few percent (cf. Refs. [30–32]). We hope that the dedicated dilepton facility HADES at GSI Darmstadt will perform such precision measurement in the near future.

VI. SUMMARY

In summary, we have calculated the ρ -meson self-energy in a pion medium at finite temperatures and charge chemical potential μ_Q , which is responsible for the difference between π^+ and π^- densities in matter. The calculation is performed within the functional integral representation for the partition function in second order of the coupling constant g_ρ^2 . We find that the pole positions and the imaginary parts of the self-energy are modified in the medium, and this modification is different for different polarization states. We show that the shift of the pole positions is probably too modest to be seen in dilepton production rates. The incorporation of a large chemical potential changes the shape of the rates, both differential and integral. Unfortunately, this effect seems to be too small for realistic values of the chemical potential μ_Q , which is expected from present relativistic

heavy-ion collision data. This means that, if the data would show strong modifications of the dielectron spectrum in the ρ mass region, it may be a signal of a more exotic physics.

Another nontrivial effect is the predicted asymmetry in the differential dielectron distribution which increases with increasing values of charged pion potential μ_Q . But we would not like to overemphasize our result because in the present stage the predicted effects have more a methodical relevance than a direct relation to experimental data. For the latter, on the one hand one has to consider the space-time evolution of the hadronic system. On the other hand, a more realistic calculation should take into account the baryonic degrees of freedom and their contribution to a complete picture. The most likely source of the large pion charge chemical potential is the neutron-proton asymmetry of the collid-

ing heavy ions. In this case, the pions are produced in a baryon-rich environment where the interaction of the ρ meson and baryons cannot be neglected. From this point of view, our relatively cumbersome calculations may be considered as a necessary step towards generalizing the vector dominance model to the case of a hot and dense nuclear isospin-asymmetric system.

ACKNOWLEDGMENTS

Useful discussions with E. Bratkovskaya, V. Lukyanov, and O. Teryaev are acknowledged. This work was supported in part by Grant No. MP8300 from the International Science Foundation and by BMBF under Grants No. 06 DR 107 and No. 06 DR 666 I(4).

-
- [1] J.J. Sakurai, *Currents and Mesons* (University of Chicago Press, Chicago, 1969).
- [2] G.J. Gounaris and J.J. Sakurai, Phys. Rev. Lett. **21**, 244 (1968).
- [3] R.D. Pisarski, Phys. Lett. **11B**, 157 (1982).
- [4] A. Gocksch, Phys. Rev. Lett. **67**, 1701 (1991).
- [5] C. Adami and G.E. Brown, Phys. Rep. **234**, 1 (1993).
- [6] G. Boyd, S. Gupta, F. Karsch, E. Laermann, B. Petersson, and K. Redlich, Phys. Lett. B **349**, 170 (1995).
- [7] A.I. Bochkarev and M.E. Shaposhnikov, Nucl. Phys. **B268**, 220 (1986); T. Hatsuda, Y. Koike, and S.H. Lee, *ibid.* **B374**, 221 (1993); M.K. Volkov and V.I. Zakharov, Yad. Fiz. **57**, 1106 (1994) [Sov. J. Nucl. Phys. **57**, 1044 (1994)].
- [8] V. Bernard and U. Meissner, Nucl. Phys. **A489**, 647 (1988); M. Jaminon, G. Ripka, and P. Stassart, *ibid.* **A504**, 733 (1989); M. Lutz, S. Klimt, and W. Weise, *ibid.* **A542**, 521 (1992); M.K. Volkov, in Proceedings of the International School-Seminar'93 "Hadrons and Nuclei from QCD" Tsuruga, Vladivostok and Sapporo, 1993, edited by K. Fujii *et al.* (unpublished), p. 238; T.I. Gulamov and A.I. Titov, Yad. Fiz. **58**, 337 (1995) [Sov. J. Nucl. Phys. **58**, 290 (1995)].
- [9] C. Gale and J.I. Kapusta, Phys. Rev. C **35**, 2107 (1987).
- [10] C.L. Korpa and S. Pratt, Phys. Rev. Lett. **64**, 1502 (1990); C.L. Korpa, L. Xiong, C.M. Ko, and P.J. Siemens, Phys. Lett. B **246**, 333 (1990); C.M. Ko, L.H. Xia, and P.J. Siemens, *ibid.* **231**, 16 (1989).
- [11] H. Herrmann, B.L. Friman, and W. Nörenberg, Z. Phys. A **343**, 119 (1992); Nucl. Phys. **A560**, 411 (1993).
- [12] C. Gale and J.L. Kapusta, Nucl. Phys. **B357**, 65 (1991).
- [13] P. Koch, Phys. Lett. B **288**, 187 (1992); Z. Phys. C **57**, 283 (1993); B. Kämpfer, P. Koch, and O.P. Pavlenko, Phys. Rev. C **49**, 1132 (1994).
- [14] M. Kataja and P.V. Ruuskanen, Phys. Lett. B **243**, 181 (1990).
- [15] J.W. Harris *et al.*, in Proceedings of the International Workshop on the Gross Properties of Nuclei and Nuclear Excitations XV, Hirschegg, Austria, 1987 (unpublished), p. 67.
- [16] E.V. Shuryak and L. Xiong, Phys. Lett. B **333**, 316 (1994).
- [17] A. Mazzoni, Nucl. Phys. **A566**, 95c (1994).
- [18] M. Gonin, Nucl. Phys. **A553**, 799c (1993).
- [19] M.I. Gorenstein and S.N. Yang, Phys. Rev. C **44**, 2875 (1991); D. Bandyopadhyay, M.I. Gorenstein, H. Stöcker, W. Greiner, and H. Sorge, Z. Phys. C **58**, 461 (1993); M.I. Gorenstein, H.G. Miller, R.M. Quick, and S.N. Yang, Phys. Rev. C **50**, 2232 (1994).
- [20] D. Pelte (private communication).
- [21] H.A. Weldon, Phys. Lett. B **274**, 133 (1992).
- [22] T.D. Cohen and W. Broniowski, INT, Univ. of Washington, Report No. DOE/ER/40561-173-INT-94-00-77 (unpublished).
- [23] T.I. Gulamov, A.I. Titov, and B. Kämpfer, FZR Rossendorf, Report No. FZR-66, December 1994 (unpublished).
- [24] C.W. Bernard, Phys. Rev. D **9**, 3312 (1974).
- [25] J.I. Kapusta, *Finite Temperature Field Theory* (Cambridge University Press, Cambridge, England, 1989).
- [26] M.B. Kislinger and P.D. Morley, Phys. Rep. **51**, 65 (1979).
- [27] C. Quigg, *Gauge Theories of the Strong, Weak and Electromagnetic Interactions* (Benjamin/Cummings, Menlo Park, CA, 1983).
- [28] C. Itzykson and J.-B. Zuber, *Quantum Field Theory* (McGraw-Hill, New York, 1980).
- [29] H.A. Weldon, Phys. Rev. D **42**, 2384 (1990).
- [30] V.D. Apokin *et al.*, Phys. Lett. B **243**, 461 (1990).
- [31] C. Ciofi degli Atti, E. Pace, and G. Salme, Phys. Rev. C **46**, R1591 (1992).
- [32] F. Frommerger *et al.*, Phys. Lett. B **339**, 17 (1994).
- [33] B. Kämpfer, O.P. Pavlenko, M.I. Gorenstein, A. Peshier, and G. Soff, Z. Phys. A **353**, 71 (1995).
- [34] T.I. Gulamov, A.I. Titov, and B. Kämpfer, FZR Rossendorf, Report No. FZR-113, November 1995 (unpublished).